

Объединенный  
институт  
ядерных  
исследований  
Дубна

1564 / 2-80

7/4-80

E1 - 12973

V.I.Komarov, G.E.Kosarev, H.Müller,  
D.Netzband, T.Stiehler, S.Tesch

**TWO-PROTON DIFFERENTIAL  
CROSS SECTIONS  
MEASURED IN PROTON-NUCLEUS  
INTERACTIONS AT 640 MeV**

**1979**



Двухчастичные дифференциальные сечения испускания протонов в протон-ядерных взаимодействиях при 640 МэВ

С целью исследования механизма эмиссии назад быстрых нуклонов в адрон-ядерных взаимодействиях измерены двухчастичные дифференциальные сечения испускания протонов в ядерных реакциях под действием протонов с энергией 640 МэВ. Измерения проведены методикой сцинтилляционных счетчиков. Экспериментальные данные сравниваются с предсказаниями каскадной модели и расчетами в рамках феноменологической модели рассеяния на нуклонных парах ядра мишени. Сделан вывод о существовании кинематической области, где эмиссия двух протонов обусловлена, в основном, квазисвободным рассеянием на скоррелированных нуклонных парах, получающих в процессе рассеяния энергию возбуждения порядка пионной массы.

Работа выполнена в Лаборатории ядерных проблем ОИЯИ.

Препринт Объединенного института ядерных исследований. Дубна 1979

Two-Proton Differential Cross Sections Measured in Proton-Nucleus Interactions at 640 MeV

Two-particle differential cross sections for fast proton emission in proton-nucleus interactions at 640 MeV are presented. The experimental data are compared with cascade model predictions and with calculations in the framework of a phenomenological model assuming scattering on nucleon pairs within the target nucleus. It has been found that there exists a kinematic region, where the two-proton emission proceeds mainly via quasifree scattering on correlated nucleon pairs.

The investigation has been performed at the Laboratory of Nuclear Problems, JINR.

Preprint of the Joint Institute for Nuclear Research. Dubna 1979

I. Nuclear reactions accompanied by emission of fast particles in backward direction are widely discussed at present. In ref.<sup>1/</sup> data on inclusive and two-particle differential cross section for proton emission in proton-nucleus collisions at 640 MeV have been published. The common criterion of the selection of events from reaction



was that at least one fast proton (notation  $p_3$ , see fig.1a) was emitted into the backward hemisphere. Coplanar measurements of two-proton correlations have been carried out using two scintillation counter telescopes with solid angles  $\Delta\Omega_1 = 19$  msr and  $\Delta\Omega_2 = 96$  msr, respectively. The energy  $T_3$  of protons  $p_3$  was measured between the values 50 and 145 MeV.

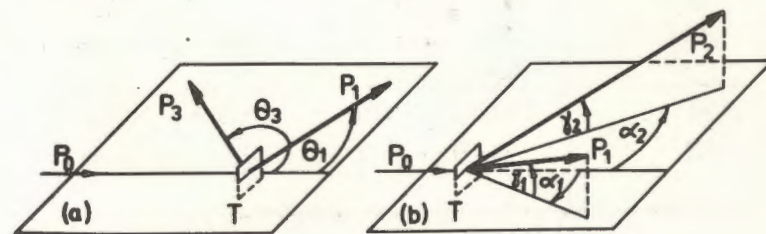


Fig.1. Geometric conditions of the measurements.  $p_0$  - incoming proton beam,  $T$  - target. (a) coplanar geometry of  $p_1$ - $p_3$  registration, (b) noncoplanar, symmetric geometry of  $p_1$ - $p_2$  registration.

Table 1

Two-proton differential cross section  $d^4\sigma/d^2\Omega dT_1 dT_3$  in units of  $\text{nb} \cdot \text{MeV}^{-2} \cdot \text{sr}^{-2}$  for reaction (1) (carbon target) in dependence on the energy  $T_3$  for two intervals of the angle  $\Theta_3$  ( $\Theta_1 = -12^\circ$ ,  $255 \text{ MeV} \leq T_1 \leq 330 \text{ MeV}$ ).

$T_3$ (MeV)	$110^\circ \dots 130^\circ$	$230^\circ \dots 250^\circ$
52	311 ± 21	126 ± 18
57	242 ± 17	100 ± 15
61	234 ± 16	128 ± 15
67	243 ± 16	113 ± 13
72	236 ± 15	76 ± 11
78	195 ± 13	72 ± 10
84	199 ± 13	67,9 ± 9,0
90	195 ± 13	62,4 ± 9,4
96	181 ± 12	28,5 ± 7,0
102	150 ± 11	48,2 ± 9,4
108	150 ± 16	25 ± 11
110	144 ± 16	52 ± 13
113	136 ± 14	27 ± 11
116	116 ± 12	21,8 ± 8,5
120	117 ± 14	32,9 ± 9,3
124	108 ± 10	20,3 ± 7,7
128	106 ± 10	14,1 ± 7,0
133	92,2 ± 8,7	16,6 ± 5,9
138	68,3 ± 6,9	10,0 ± 5,6
143	62,0 ± 6,5	14,9 ± 5,1

The protons  $p_1$  were registered within the energy interval  $255 \text{ MeV} \leq T_1 \leq 330 \text{ MeV}$ . Therefore, the differential cross sections presented in tables 1-3 and 5 are mean values for this energy interval  $T_1$ , and the cross sections given in table 4 are mean values for the  $T_1$  energy interval given there.

Table 2

Two-proton cross section I for process (1) (carbon target) in dependence on the backward angle  $\Theta_3$  for three  $T_3$  energy intervals ( $\Theta_1 = -12^\circ$ ,  $255 \text{ MeV} \leq T_1 \leq 330 \text{ MeV}$ ).

$\Theta_3$ (deg)	cross section I ( $\text{nb} \cdot \text{MeV}^{-2} \cdot \text{sr}^{-2}$ )		
	50 ... 90 MeV	105 ... 145 MeV	50 ... 145 MeV
105	233 ± 30	157 ± 19	196 ± 18
110	254 ± 28	164 ± 19	211 ± 18
115	268 ± 26	120 ± 13	192 ± 16
120	244 ± 23	113 ± 11	179 ± 14
122	223 ± 21	106 ± 10	165 ± 12
130	203 ± 22	63 ± 9	133 ± 13
140	175 ± 17	50 ± 6	112 ± 10
150	162 ± 18	36 ± 6	95 ± 9
155	142 ± 17	33 ± 6	86 ± 9
205	73 ± 10	18 ± 5	44 ± 6
210	70 ± 11	19 ± 4	44 ± 6
220	82 ± 10	19 ± 4	48 ± 5
230	74 ± 9	27 ± 4	49 ± 5
240	92 ± 13	10 ± 5	48 ± 7
245	102 ± 11	21 ± 4	60 ± 6
250	110 ± 13	33 ± 6	70 ± 7
255	113 ± 18	42 ± 8	75 ± 9

The cross sections

$$I = \frac{1}{T_{3 \text{ max}} - T_{3 \text{ min}}} \int_{T_{3 \text{ min}}}^{T_{3 \text{ max}}} \frac{d^4\sigma}{d^2\Omega dT_1 dT_3} dT_3$$

in tables 2-5 are given for three energy intervals of the backward emitted proton  $p_3$ . The absolute error of the data normalization has been estimated to amount to 20%.

Table 3

Two-proton cross section I in dependence on the forward angle  $\Theta_1$  ( $\Theta_3 = 122^\circ$ ,  $255 \text{ MeV} \leq T_1 \leq 330 \text{ MeV}$ , carbon target).

$\Theta_1$ (deg)	cross section I ( nb $\cdot$ MeV $^{-2}$ $\cdot$ sr $^{-2}$ )		
	50 ... 90 MeV	105 ... 145 MeV	50 ... 145 MeV
- 40	47,8 $\pm$ 5,9	16,7 $\pm$ 3,1	31,2 $\pm$ 3,2
- 30	80,8 $\pm$ 8,4	28,7 $\pm$ 4,0	53,2 $\pm$ 4,6
- 20	135 $\pm$ 14	60,2 $\pm$ 7,4	99,3 $\pm$ 8,4
- 15	201 $\pm$ 20	84,1 $\pm$ 9,6	144 $\pm$ 12
- 12	223 $\pm$ 21	105,8 $\pm$ 9,7	165 $\pm$ 12
- 10	258 $\pm$ 32	76 $\pm$ 13	163 $\pm$ 17
- 8	370 $\pm$ 140	166 $\pm$ 43	267 $\pm$ 71
8	95 $\pm$ 84	67 $\pm$ 27	75 $\pm$ 41
10	116 $\pm$ 21	14,9 $\pm$ 9,4	63 $\pm$ 11
15	56,6 $\pm$ 8,7	14,7 $\pm$ 4,1	34,3 $\pm$ 4,6
20	46,5 $\pm$ 6,8	7,5 $\pm$ 2,3	25,3 $\pm$ 3,3
30	- 1,0 $\pm$ 1,3	1,0 $\pm$ 0,9	-0,1 $\pm$ 0,7
40	8,9 $\pm$ 2,0	1,1 $\pm$ 1,7	4,1 $\pm$ 1,2

In ref.<sup>1/</sup> it has been shown that in contrast to the one-particle cross sections those of two-nucleon emission cannot be described in the framework of the cascade model<sup>2/</sup>: The calculated contributions to the experimentally observed yields do not exceed about 20% in the essential part of the investigated kinematic region.

We suppose now that the main contribution to the  $p_1 - p_3$  cross sections is due to the quasifree scattering on correlated nucleon pairs according to



Such a scattering process is not included in the cascade model calculations, and the usual cascade mechanisms fail in reproducing the two-proton emission according to process (2). Indeed, elastic scatterings on uncorrelated nucleons with

Table 4

Two-proton cross section I in dependence on the proton energy  $T_1$  ( $\Theta_1 = -12^\circ$ ,  $\Theta_3 = 122^\circ$ , carbon target).

$T_{1\text{min}}$ (MeV)	$T_{1\text{max}}$ (MeV)	cross section I (nb $\cdot$ MeV $^{-2}$ $\cdot$ sr $^{-2}$ )		
		50 ... 90 MeV	105 ... 145 MeV	50 ... 145 MeV
141	210	220 $\pm$ 23	103 $\pm$ 10	162 $\pm$ 13
172	236	233 $\pm$ 24	106 $\pm$ 12	170 $\pm$ 14
197	255	240 $\pm$ 23	103 $\pm$ 11	170 $\pm$ 13
221	275	244 $\pm$ 23	89,4 $\pm$ 9,3	164 $\pm$ 12
250	301	268 $\pm$ 26	107 $\pm$ 12	186 $\pm$ 15
265	308	330 $\pm$ 33	128 $\pm$ 15	230 $\pm$ 19
286	327	314 $\pm$ 32	109 $\pm$ 14	209 $\pm$ 18

a momentum distribution of noninteracting Fermi particles cannot explain the emission of fast protons near  $180^\circ$  (see refs.<sup>1,3/</sup>). Further, the mechanism of intranuclear absorption of pions<sup>3/</sup> produced during the cascade development requires in contrast to scattering (2) that at least three nucleons of the target nucleus effectively take part in the reaction (one nucleon for the production of the pion and a pair of correlated nucleons for the  $\pi$ -absorption).

2. If the emission of fast nucleons really is due to process (2) then in agreement with the kinematics of this process the knockout of fast nucleon pairs  $p_1 - N_2$  into the forward direction should be expected. In table 6 we present differential cross section data of two-proton forward emission.

Protons  $p_1$  and  $p_2$  have been registered within the energy interval  $265 \text{ MeV} \leq T_1(T_2) \leq 340 \text{ MeV}$  using two identical scintillation counter telescopes with solid angles  $\Delta\Omega_{1(2)} = 7 \text{ msr}$ . In order to reduce the detector loads at small angles the telescope axes were adjusted at angles  $\gamma_1 = \gamma_2 = 12^\circ$  with respect to the plane containing the beam axis (see fig.1b). Pion registration was suppressed by using threshold Cerenkov counters. The background of random events and that without target have also been measu-

Table 5

Two-proton yield measured with different targets ( $\Theta_1 = -12^\circ$ ,  $\Theta_3 = 122^\circ$ ,  $255 \text{ MeV} \leq T_1 \leq 330 \text{ MeV}$ ).

target	cross section I (nb . MeV <sup>-2</sup> . sr <sup>-2</sup> )		
	50 ... 90 MeV	105 ... 145 MeV	50 ... 145 MeV
Be	180 ± 17	85 ± 9	133 ± 11
C	219 ± 20	92 ± 9	154 ± 12
Al	343 ± 33	125 ± 14	231 ± 19
Cu	625 ± 62	203 ± 23	403 ± 34
Pb	608 ± 73	242 ± 35	412 ± 41

Table 6

Differential cross section I of forward emitted protons of reaction (1) in dependence on the angle  $\alpha$  ( $\alpha \equiv \alpha_1 = \alpha_2$ ,  $\gamma_1 = \gamma_2 = 12^\circ$ ,  $265 \text{ MeV} \leq T_1(T_2) \leq 340 \text{ MeV}$ , carbon target).

$\alpha$ (deg)	I (nb . MeV <sup>-2</sup> . sr <sup>-2</sup> )
5,7	103 ± 16
7,5	61 ± 26
10	43 ± 39
12	45 ± 23
14	16 ± 26
16	20 ± 13
20	49 ± 13
25	82 ± 22
30	150 ± 18
35	187 ± 22
40	211 ± 16

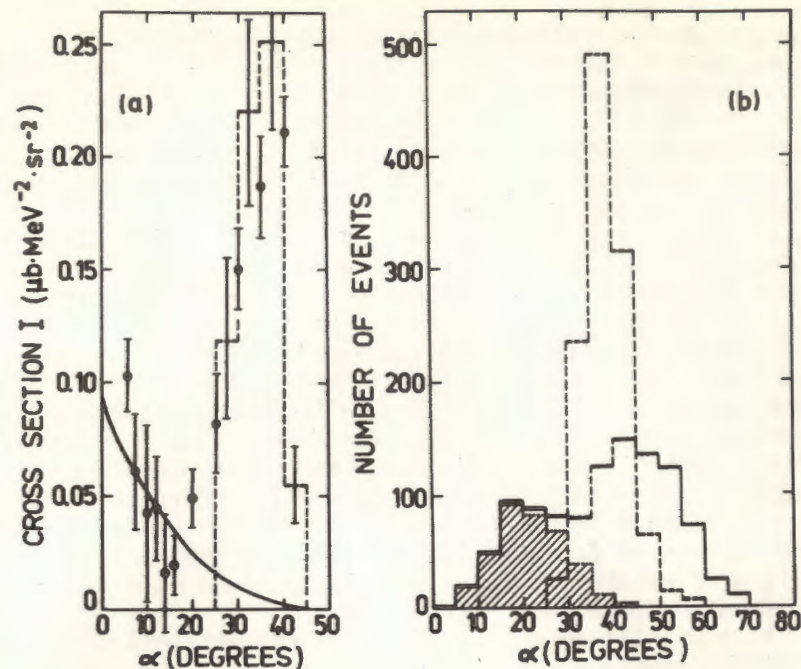


Fig.2. (a) Two-proton angular distribution measured in non-coplanar symmetric geometry (carbon target). Points - experiment; histogram - cascade model calculation; full line - calculation with the model described in the text and normalized to the experimental cross section at  $7.5^\circ$ . (b) Cascade model predictions of two-proton events (coplanar geometry). Dashed line - energy window  $265 \text{ MeV} \leq T_1(T_2) \leq 340 \text{ MeV}$ ; full line - at least one proton within energy window  $190 \text{ MeV} \leq T \leq 265 \text{ MeV}$ ; hatched region - contribution from events with intranuclear pion production.

red and were taken into account in the data processing. A more detailed description of the experimental arrangement can be found in refs.<sup>1,4/</sup>.

3. The differential cross sections  $I = d^4\sigma / d^2\Omega dT_1 dT_2$  given in table 6 are mean values with respect to the energy intervals  $T_1$  and  $T_2$  of the detected protons. The measu-

rement was carried out in symmetric geometry, i.e.,  $a_1 = a_2 (= a)$ . As is seen in fig.2a, the cross section  $I(a)$  is characterized by a steep increase in the angular interval from  $20^\circ$  to  $40^\circ$ . Such an increase is obviously due to the registration of protons from the  $(p, 2p)$  quasielastic scattering. It is known (see, e.g., ref.<sup>15/</sup>) that in accordance with the elastic NN kinematics the coplanar  $(p, 2p)$  knock-out process has its maximum near  $a = 41^\circ$ , and this peak is spread by the Fermi motion of the target nucleons. However, the increase of the two-proton yield seen clearly at small angles  $a$  cannot be explained by the quasielastic scattering on single nucleons. Indeed, as is shown in fig.2a, this scattering process calculated in the framework of the cascade model does not contribute to the small-angle cross section. Under the kinematic condition of the  $p_1-p_2$  experiment cascade events involving inelastic intranuclear NN collisions are suppressed in consequence of the high energetic thresholds for proton registration. Cascade events at small  $a$  can be produced only by lowering the energy window of proton detection, where the intranuclear pion production becomes possible (see fig.2b).

4. The small-angle two-proton cross section can be described by using a phenomenological model in which a scattering mechanism on correlated nucleon pairs according to process (2) is assumed. In order to express the tendency of forward scattering of the incoming proton and excitation of the nucleon pair the reaction amplitude  $A$  is used in the following form:

$$|A|^2 = \exp[-(\theta_{01} p_0 a_{ch})^2 - E_{23}/E_{ch}] + \exp[-(\theta_{02} p_0 a_{ch})^2 - E_{13}/E_{ch}]. \quad (3)$$

Here the parameter  $a_{ch}$  characterizes the linear dimension of a volume occupied by the nucleon pair in the target, and  $E_{ch}$  gives the probability for the excitation of the  $[NN]$  - cluster to energy  $E_{ij} = M_{ij}^{inv} - 2m_N$  (here  $M_{ij}^{inv}$  means the invariant mass of the nucleon pair  $p_i p_j$  in the final state of process (2) and  $m_N$  is the nucleon mass).

The calculations were carried out by using the Monte Carlo method. The Fermi motion of the nucleon pair was considered, but wave distortions in the initial and final states of the reaction were not taken into account.

The result of calculation with parameter values  $a_{ch} = 0.5$  fm and  $E_{ch} = m_\pi = 0.14$  GeV is shown in fig.2a. It has been found that the Fermi motion of the  $[NN]$ -group has only a weak influence on the distribution. The result depends also weakly on the parameter  $E_{ch}$ , because in the kinematic region considered the variables  $E_{23}$  and  $E_{13}$  change not strongly: from 272 MeV at  $a = 7.5^\circ$  to 194 MeV at  $32^\circ$ . Only the parameter  $a_{ch}$  turns out to be important. Its value must be taken between 0.3 fm and 0.7 fm in order to reproduce the experimentally observed increase of the cross section at small angles.

We remark that the proposed model assuming cluster excitation is also capable of reproducing the main peculiarities of  $p_1-p_3$  data (see ref.<sup>1/</sup>). The normalization factors of the reaction amplitude for process (2) found by comparing the calculated and the experimental cross sections turn out to be similar for  $p_1-p_2$  and  $p_1-p_3$  distributions as well. For the  $p_1-p_2$  measurement such normalization factor is about four times larger than for the  $p_1-p_3$  data, but stronger absorption of the proton  $p_3$  in the final nucleus partly compensates this difference. Therefore also the absolute values of the measured differential cross sections indicate that the dominating mechanism of two-proton emission in the cases under study are alike.

It seems justifiable to assume that this mechanism is connected with relatively large momentum transfer to the nucleon pair at our experimental conditions. The invariant momentum transfer  $\sqrt{|t_{01(2)}|}$  between the protons  $p_0$  and  $p_{1(2)}$  changes from  $1.7 \text{ fm}^{-1}$  at  $a = 7.5^\circ$  to  $3.2 \text{ fm}^{-1}$  at  $32^\circ$ , exceeding values of the order  $h/\bar{l}_{NN}$ , where  $\bar{l}_{NN}$  is the mean intranuclear distance between the nucleons.

We conclude that in our two-particle measurements a kinematic region has been chosen, in which the interaction of medium-energy protons with light nuclei proceeds mainly via the quasifree scattering on intranuclear two-nucleon groups.

We are indebted to K.K.Gudima and S.G.Mashnik for fruitful discussions concerning the cascade model calculations.

#### REFERENCES

1. Komarov V.I., et al. Nucl.Phys., 1979, A326, p.297.
2. Barashenkov V.S., et al. Nucl.Phys., 1972, A178, p.531.
3. Gudima K.K., Mashnik S.G., Toneev V.D. JINR, E2-11307, 1978.

4. Komarov V.I., et al. JINR, P13-9638, 1976.
5. Jacob G., Maris Th.A.J. Rev.Mod.Phys., 1973, 45, p.6;  
Pedrisat C.F., et al. Phys.Rev., 1969, 187, p.1201.

Received by Publishing Department  
on December 3 1979.